SHIPBOARD INFRARED CIRCULAR POLARIZATION SENSOR FOR SEA-SKIMMING MISSILE DETECTION

December 1999

T. W. Nee and S. F. Nee
Naval Air Warfare Center Weapons Division
China Lake, CA 93555-6100
Phone: (760) 939-8225
Email: neet@navair.navy.mil

ABSTRACT

A circular polarization sensor is feasible to detect a sea-skimming cruise missile in a solar corridor. We report the simulated performance results of a shipboard medium-wave infrared (MWIR) circular polarization sensor to detect a sea-skimming missile above rough sea surface. The sensor observed total and circular target and sea clutter signals at night and during daytime in and out of the solar corridor. The simulation model includes (1) Cox Munk rough sea slope distribution, (2) missile target with cylindrical body, conic nose, and cylindrical plume surfaces, (3) published in-band optical constants of water and painted target, and (4) the radiation sources—(i) thermal emission from target/sea surface, (ii) reflection of atmospheric and sun glints radiation, and (iii) scattered light from rough sea surface. The in-band target vs. sea-clutter irradiances are plotted for horizontal range between 5 and 30 km. This plot provides a quantitative basis to determine the required sensor sensitivity—noise equivalent irradiance (NEI)—of a MWIR circular polarization sensor. Our model full-polarization sensor parameters are feasible for detecting sea-skimming missiles in and out of the solar corridor and at night.

I. INTRODUCTION

Either linear or circular polarization is a fundamental property of radiation and is a well-understood phenomenon. The imaging profiles and signatures of man-made targets are polarization-dependent. Natural background clutter and plume signatures are mostly unpolarized or have very different polarization characteristics from those of the targets. Based upon this fact, polarization-based imaging of targets in clutter and background has received increasing attention since it can provide more discrimination power than simple intensity imaging[1].

The polarization state of light can be completely described by four Stokes parameters, I, Q, U, and V. Q and U are the two independent linear polarization intensities and V is the circular polarization intensity. They have the same dimension as intensity I. A full-polarization sensor is a sensor that can detect I, Q, U, and V simultaneously.

As shown in Figure 1, current electro-optical infrared (EO/IR) intensity-only I-sensors are significantly compromised by solar glints and sea clutter (saturation issues, false alarms, etc.) when looking into the solar corridors and, therefore, are not effective for detecting and tracking critical threats such as sea-skimming cruise missiles.

[1] M. R. Hess, G. A. Freund, D. L. McMaster, D. B. Nichols, M. A. LeCompte, F. J. Iannarilli, and J. E. Rice. "Measurement and Analysis of Aircraft Infrared Signature Polarization," in *IRIA-IRIS Proceedings: 1994 Meeting of the IRIS Specialty Group on Targets, Backgrounds and Discrimination*, Vol. IV (September 1994), pp. 207-226.

Report Documentation Page

Report Date	Report Type	Dates Covered (from... to)
00121999	N/A	-

Title and Subtitle Shipboard Infrared Circular Polarization Sensor for Sea-Skimming Missile Detection	**Contract Number**
	Grant Number
	Program Element Number
Author(s) Nee, T. W.; Nee, S. F.	**Project Number**
	Task Number
	Work Unit Number
Performing Organization Name(s) and Address(es) Naval Air Warfare Center Weapons Division China Lake, CA 93555-6100	**Performing Organization Report Number**
Sponsoring/Monitoring Agency Name(s) and Address(es) Director, CECOM RDEC Night Vision and Electronic Sensors Directorate, Security Team 10221 Burbeck Road Ft. Belvoir, VA 22060-5806	**Sponsor/Monitor's Acronym(s)**
	Sponsor/Monitor's Report Number(s)
Distribution/Availability Statement Approved for public release, distribution unlimited	
Supplementary Notes The original document contains color images.	
Abstract	
Subject Terms	
Report Classification unclassified	**Classification of this page** unclassified
Classification of Abstract unclassified	**Limitation of Abstract** UNLIMITED
Number of Pages 15	

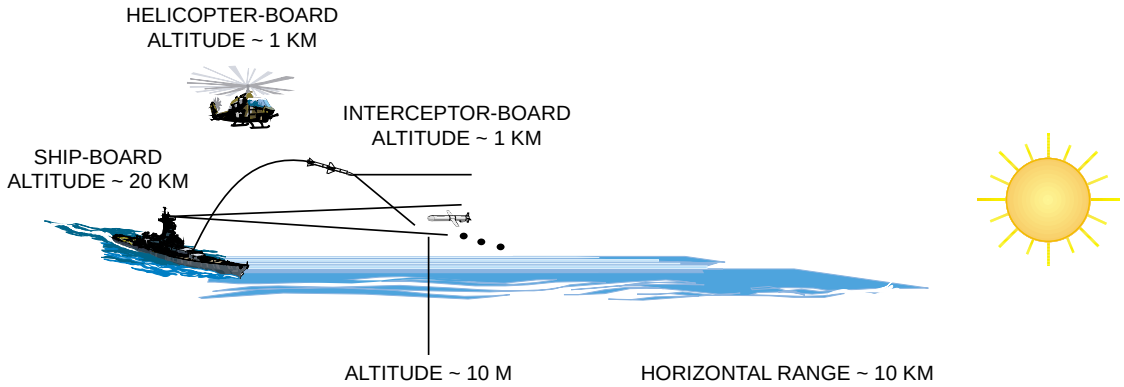

Figure 1. EO/IR Sensors to Detecting Sea-Skimming Target Geometry in the Solar Corridor.

We analyzed the performance of an infrared passive polarization sensor for discrimination applications using a full-polarization sensor. The results showed the application feasibility for (1) target/debris/altitude control module (ACM) discrimination of Ballistic Missile Defense (BMD) using linear polarization and (2) detection of a sea-skimming missile in the presence of sea clutter and solar background using circular polarization[2,3,4,5,6,7]. The application of linear polarization imaging (Q, U) for real-target/background discrimination and mines-target identification was also demonstrated[1,8]. Nichols Research (NRC) recently developed a full-polarization Stokes (I, Q, U, V) medium-wave infrared (MWIR) imager and demonstrated target-littoral background discrimination. The strong circular littoral background scenes were first demonstrated[9]. Therefore, a circular-polarization sensor for military application would be a promising research/development field.

For a sea-skimming missile in the solar corridor, the solar radiation reflected from the sea surface and then from the missile surface would have a significant circular component. However, the background of solar radiation reflected from the sea would have a negligibly small circular component (it is zero for a flat water surface)[4,7]. These phenomena can be used to detect a sea-skimming missile in the presence of sea clutter and solar background. The rough sea surface would also generate a circular polarization background. In this paper, we include the effects of atmospheric absorption and the rough sea surface. For comparison with the performance of existing I-sensors, a more realistic model of the target and sea background would be used for analysis and simulation.

The fundamental theory of full-polarization signatures was reported[2,3,4] and is not repeated here.

---

[2] Tsu-Wei Nee, and Soe-Mie F. Nee. "Infrared polarization signatures for targets," *Proc. SPIE **2469***, April 1995, pp. 231-241.

[3] T. W. Nee, J. Bevan, J. Bobinchak, and S. F. Nee. "Infrared Polarization Signatures for Target/Background," *Proceeding of Workshop on Infrared and Millimeter Wave Polarimetry 5-7 December 1995*. Redstone Arsenal, Ala., April 1996, pp. 163-181.

[4] T. W. Nee, S. F. Nee and E. J. Bevan. "Infrared Polarization Signatures of a Target for Enhanced Discrimination," in *IRIA-IRIS Proceedings: 1996 Meeting of the IRIS Specialty Group on Targets, Backgrounds and Discrimination*. Vol. **IV** (October 1996), pp. 349-368.

[5] T. W. Nee, S. F. Nee and E. J. Bevan. "Infrared Polarization Imaging Sensor for TBMD Discrimination and Tracking," *The Second Theater Missile Defense Critical Measurements Program Data Analysis Workshop Proceedings*. Vol. III, MIT Lincoln Laboratory, Massachusetts, 22-24 January 1997, pp. 1379-1399.

[6] T. W. Nee, S. F. Nee and E. J. Bevan, "Dual-mode Electro-optical Polarization Sensor For Surveillance And Discrimination The 7th AIAA/BMDO Technology Readiness Conference, August 3-7 1998, Ft. Carson and Colorado Springs, CO (SECRET).

[7] T. W. Nee, S. F. Nee and E. J. Bevan, "Infrared Circular Polarization Sensor For Sea-Skimming Missile Detection *1998 National Fire Control Symposium, Theater Air Defense, NAVSEA, 3 - 6 August 1998*, San Diego, CA.

[8] L. Cheng, and G. Reys. "AOTF Polarimetric Hyperspectral Imaging for Mine Detection," *Proc. SPIE **2496***, Orlando, Fla., April 1995, pp. 305-311.

[9] Blair Barbour, "Clutter Discrimination Polarization, CLEAR Sensor Technology". Nicholes Research Proprietary 16198-00/1904, June 1998.

II. CIRCULAR-POLARIZATION REFLECTION—REFLECTION FROM THE OF A CYLINDRICAL TARGET ABOVE—SEA SURFACE IN SOLAR CORRIDOR

In the model calculation, we consider only the major solar radiation source and neglect other radiation contributions. The effects of atmospheric absorption and rough sea surface are included. The atmospheric absorption and the solar radiation spectra have the major effect for band selection. The rough water surface would produce non-vanishing circular background. As shown in Figure 2 (ray 2), the total intensity of the cylindrical skimmer toward the sensor is

$$I_j = \int dS_n \int_{\lambda_{min}}^{\lambda_{max}} d\lambda \, [RR_W]_j \, W_S(\lambda, T_S) / \Omega_S \qquad (j = I, Q, U, V) \tag{1}$$

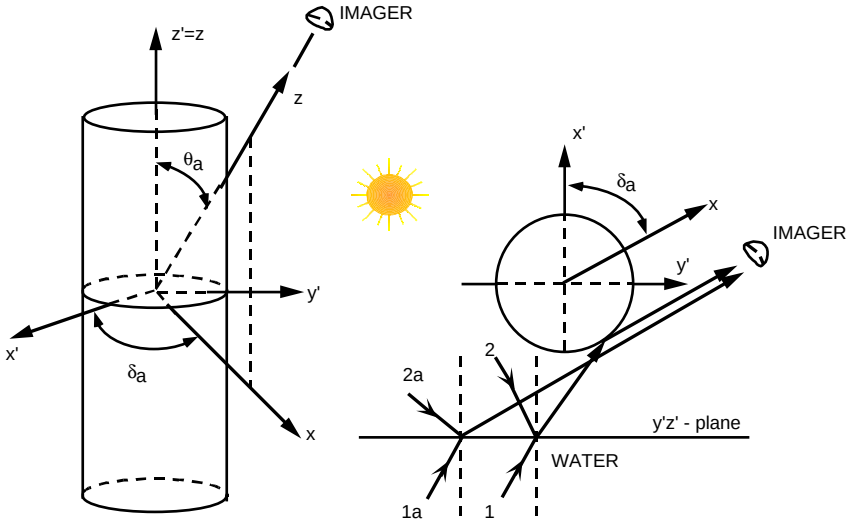

Figure 2. The Observation Geometry of a Cylinder Above the Water Plane.

where T_S = 6000 K is the solar temperature, $W_S(\lambda,T_S)$ is the solar spectral irradiance at sea surface[10] and is shown in Figure 3 for the MWIR band. $[RR_W]_j$ are the effective reflectance coefficients attributable to the double reflections of water $[R_W]$ and missile surface [R]. Ω_S = 6.3E-3 Str is the solid angle of solar disk. For the target at range Rg, the irradiance onto the sensor is

$$E_j = \tau(R_g)\frac{I_j}{R_g^2} \tag{2}$$

[10] E. E. Bell, L. Eisner, J. Young, R. A. Oetjen. "Spectral Radiance of Sky and Terrain at Wavelengths Between 1 and 20 Microns. II. Sky Measurements," *J. Opt. Soc.* Am **50,** pp. 1313-1320 (1960).

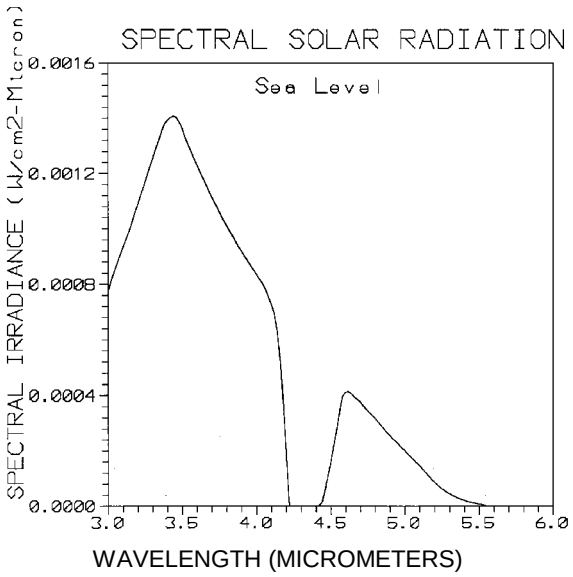

Figure 3. The MWIR Solar Spectral Irradiance at Sea Surface.

$\tau(R_g)$ is the spectrally $[\lambda_{min},\lambda_{max}]$ averaged atmospheric transmission coefficient between the target and the sensor. The total radiant intensity of the water-reflected solar radiation toward the sensor is

$$I_{wj} = \int dS_n \int_{\lambda_{min}}^{\lambda_{max}} d\lambda \left[R_w\right]_j W_S\left(\lambda, T_S\right) / \Omega_S \qquad (j = I, Q, U, V) \tag{3}$$

$[R_w]_j$ are the effective reflectance coefficients of water surface. For the water surface at range R_g, the irradiance onto the sensor (ray 2a of Figure 2) is

$$E_{wj} = \tau\left(R_g\right)\frac{I_{wj}}{R_g^2} \tag{4}$$

FLAT-WATER-PLANE MODEL

We consider a cylindrical target model 10 m long, 0.5 m radius, and 10 m above a water plane (XY-plane) as shown in the Figure 4. It is located at a distance X km from the YZ-plane and with its axis in the XZ-plane and along the X-direction. The sensor at two positions is studied: (1) a shipboard sensor located in the YZ-plane, at a distance 100 m from the XZ-plane and an altitude 20 m above the water surface, and (2) an interceptor helicopter-board sensor located in the YZ-plane, at a distance 2 km from the XZ-plane and an altitude 1 km above the water surface. The situation is shown in Figure 1. We assume that the water-reflected solar glint toward the sensor has spread incident angles of (1) 10-degree range (79.95 to 89.95 degrees) and (2) 40-degree range (49.95 to 89.95 degrees), respectively. We assume that the target surface is made from a painted surface with optical constants 1.5 + i 0.15[11], and the water has optical constants 1.374 + i0.0036 (at wavelength 3.7 μm)[12].

[11] S. F. Nee, P. C. Archibald, J. M. Bennett, D. K. Burge, and T. W. Nee. "Polarization by Rough Painted Surfaces," *Proceeding of Workshop on Infrared and Millimeter Wave Polarimetry 5-7 December 1995*. Redstone Arsenal, Ala., April 1996, pp. 527-542.

[12] G. M. Hale, and M. R. Querry, "Optical Constants of Water in the 200-nm to 200-μm Wavelength Region", Appl. Optics, **12**, pp. 555-563 (1973).

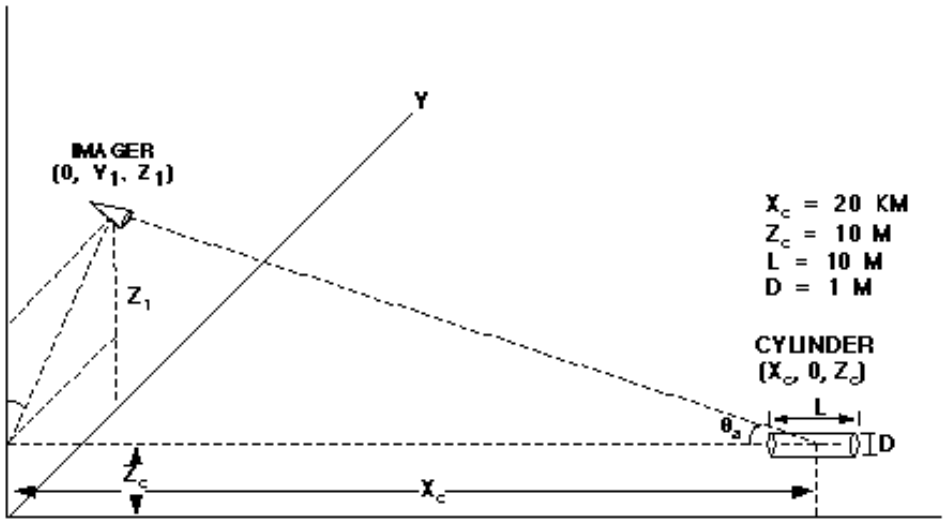

Figure 4. A Model Geometry of the Imaging Sensor and a Cylindrical Target Above a Flat Water Plane.

For the case of flat water surface, the irradiances of I-, V-, and water background I- signatures (MWIR 3.3- to 3.7-μm band) are calculated and shown in Figure 5. In this geometry, the strong water-reflected solar glint exists for a horizontal range X > 2 km. In this solar corridor, the target I-irradiance is much smaller than the water-reflected solar I-background. Taking the sensor MDI = 10 fW/cm^2, the circular component target signatures are measurable and have acquisition ranges of 16.2 and 56.8 km for positions 1 and 2, respectively. The 3.3- to 3.7-μm band is a near optimum choice of the greatest spectral signature of solar radiation source near the sea surface (Figure 3).

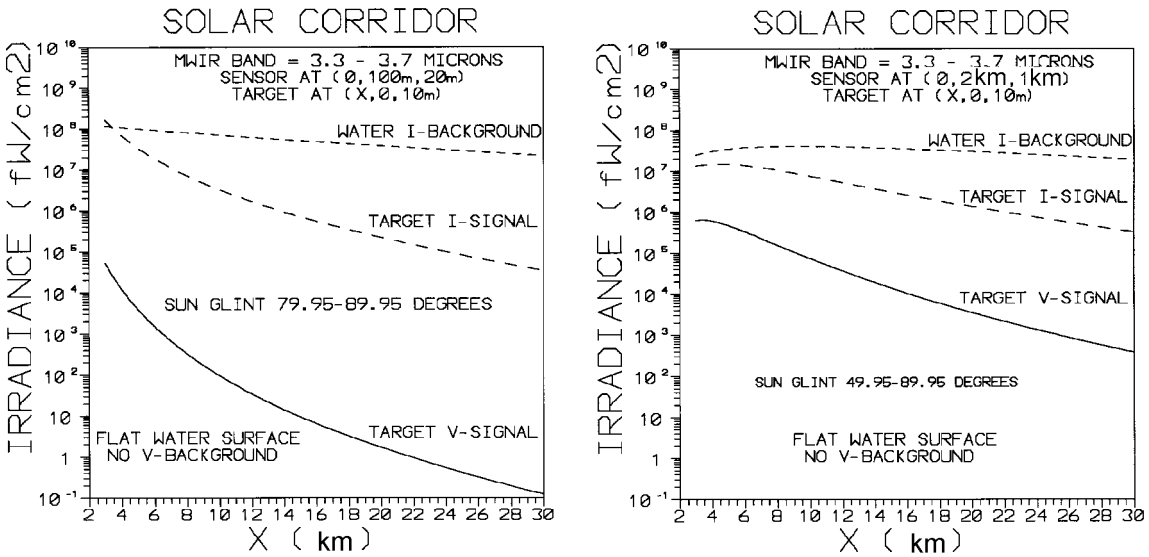

Figure 5. The MWIR Irradiances of Solar Glints From (1) I- and V- Reflection-Reflection the Model Cylindrical Target and (2) the I-Reflection of Water Background in Solar Corridor. The sensors are at (1) [0, 100 m, 20 m] and (2) [0, 2 km, 1 km]. Flat water surface is assumed.

ROUGH-SEA-SURFACE MODEL

The double reflection of unpolarized solar radiation from two surfaces would generate circular-component radiation with a nonvanishing V signature. Then the nonvanishing V-component of rough-sea background is expected. This effect will limit the application potential of sea-skimmer detection in the solar corridor. We make a study of the strength.

A model based upon double reflection[13] for a rough-surface backscattering was developed[14]. Using the sea-surface distribution of Cox-Munk model[15], the polarization properties of double-reflection surface scattering (effective Mueller matrix and the MWIR—I, Q, U, V) signatures of the reflected solar background from a rough-water surface are calculated. The degrees of circular (V/I) and linear (I_{lp}/I) polarizations are calculated. The results for the near grazing cases (incident angles greater than 80 degrees) for sea surfaces with wind speeds of 0, 2.5, 5, and 10 m/s are shown in Figure 6. Figure 6 shows that the circular-polarization signal (V) is less than 1E-6 of the intensity signal (I) near the horizon (incident angle > 89 degrees).

For the two sensors at positions 1 (0, 100 m, 20 m) and 2 (0, 2 km, 1 km), the I-, V-irradiances of target and water background (MWIR 3.3- to 3.7-μm) are calculated. The results for sea-surface wind speeds of 0 and 10 m/s are calculated and shown in Figures 7 and 8. The ratio E_V/E_{VW} is calculated and also shown in Figure 9.

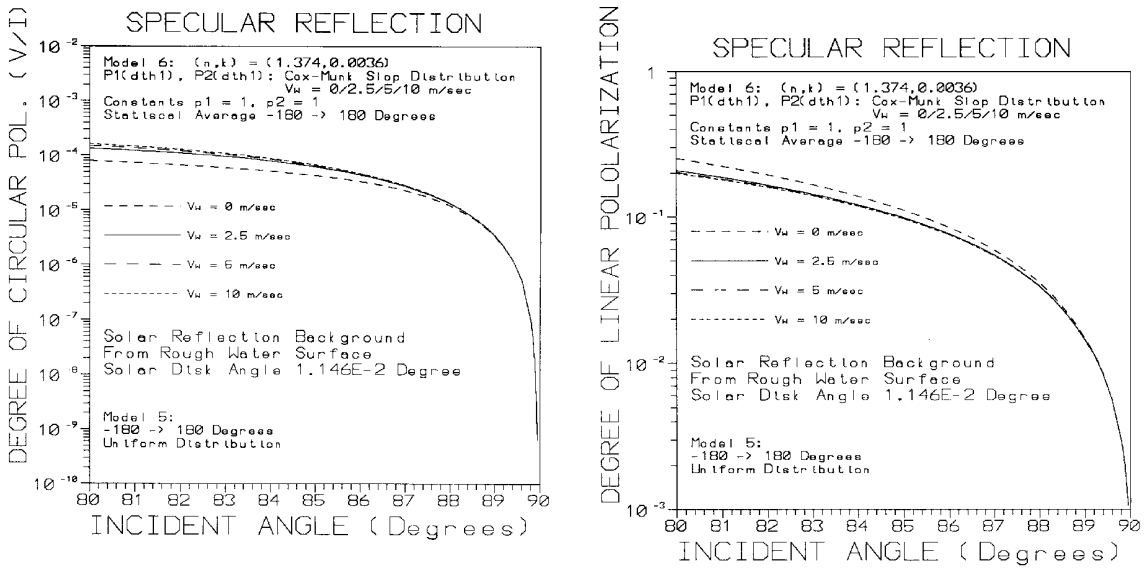

Figure 6. Polarization Background of Water Reflection. The degrees of circular (V/I) and linear (I_{lp}/I) polarizations for the near grazing cases with incident angles greater than 80 degrees. Results for sea surfaces with wind speeds of 0, 2.5, 5, and 10 m/s (Cox-Munk model) are shown.

[13] Z. H. Gu, J. Q. Lu and M. M. Tehrani. "Enhanced Backscattering of Polarized Light at Vacuum/Dielectric Interfaces," *Optical Eng*, 34, pp. 1611-1624 (1995).

[14] T. W. Nee, and S. F. Nee. "Polarization Theory of Rough Surface Scattering," (In preparation).

[15] C. Cox, and W. Munk. "Measurement of Roughness of the Sea Surface From Photographs of the Sun's Glitter," *J. Opt. Soc.* Am **44,** pp. 838-850 (1954).

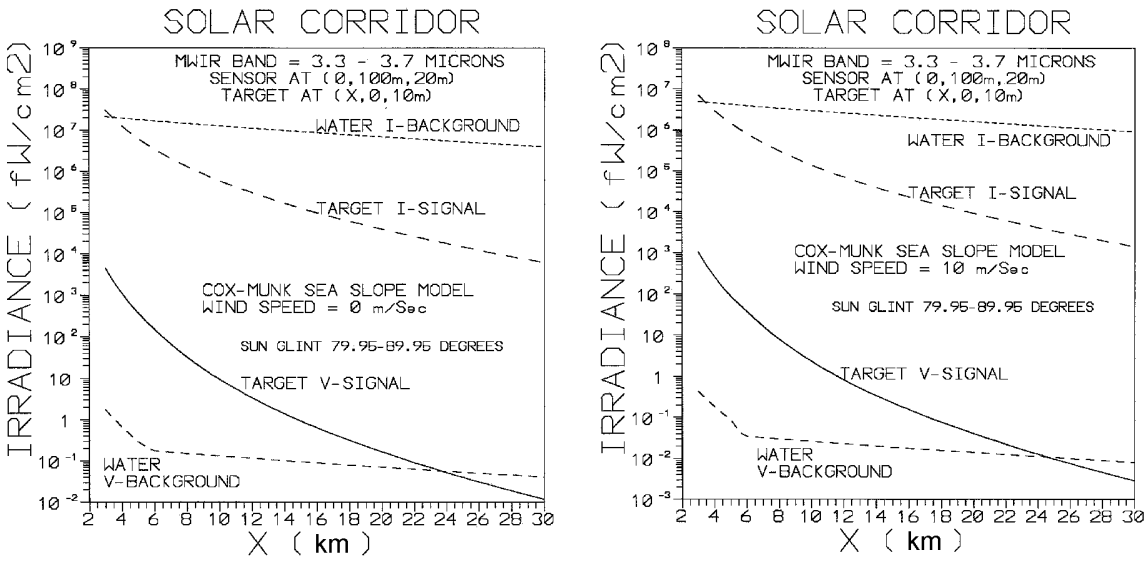

Figure 7. For the Sensor at Position 1, the MWIR Solar Glints Generated I- and V-Irradiances of the Model Cylindrical Target and That of Water Background in Solar Corridor. Results for sea surfaces with wind speeds of 0 and 10 m/s (Cox-Munk model) are shown.

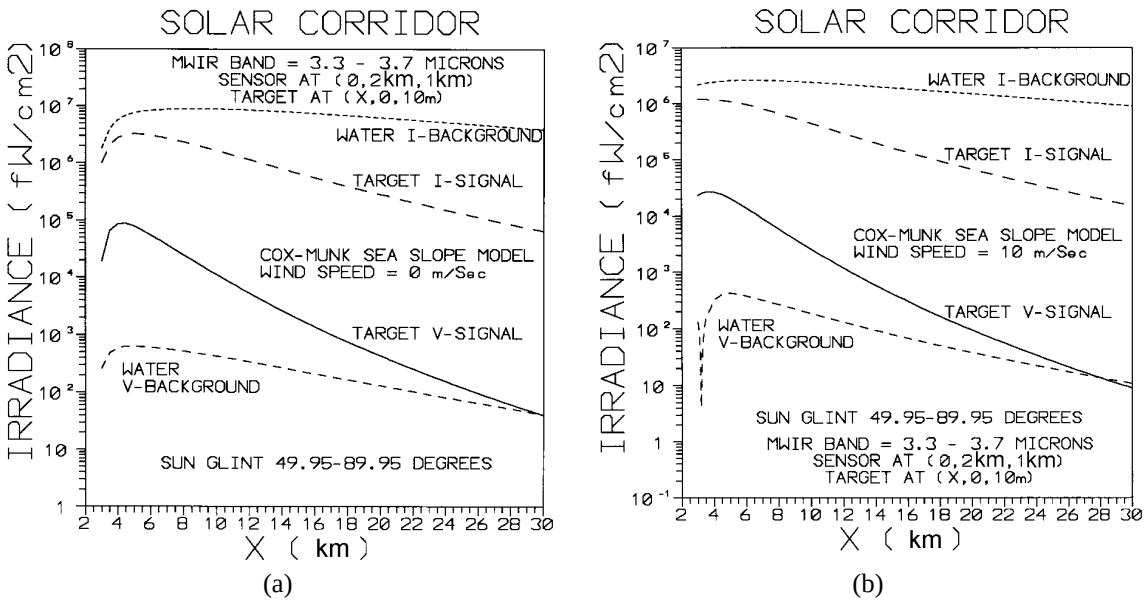

Figure 8. For the Sensor at Position 2, the MWIR Solar Glints Generated I- and V-Irradiances of the Model Cylindrical Target and That of Water Background in the Solar Corridor. Results for sea surfaces with wind speeds of 0 and 10 m/s (Cox-Munk model) are shown.

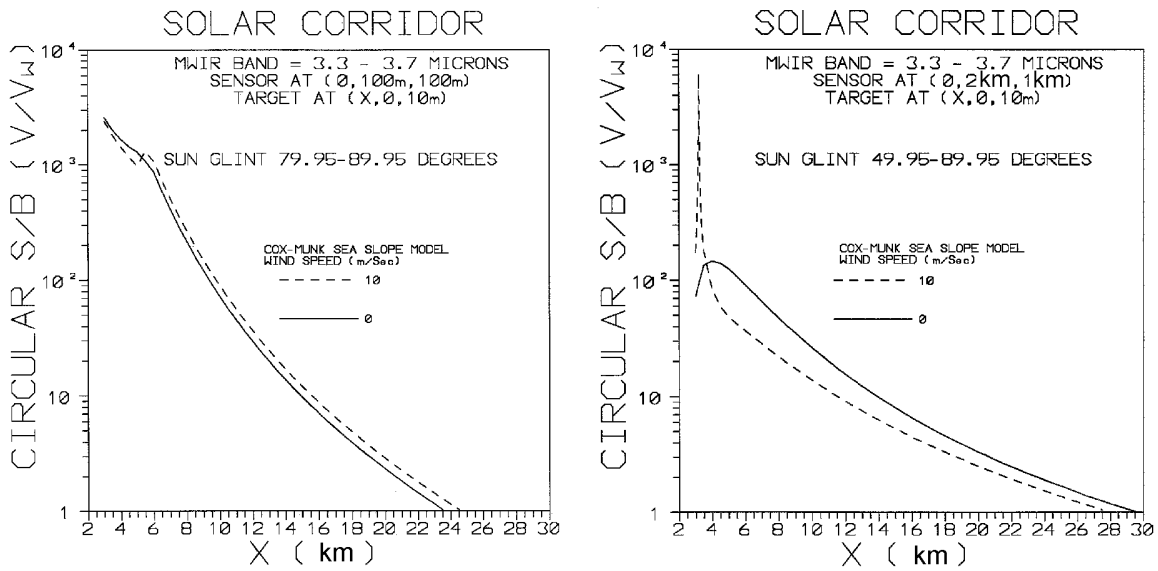

(a) (b)

Figure 9. For the Sensor at Positions 1 and 2 and in the Solar Corridor (Figures 7 and 8), the Circular Polarization Signal to Clutter Ratio V/V_W.

The relation E_V/E_{VW} versus E_V for the sensor at position 1 is shown in Figure 10. If we take the sensor MDI to be 10 fW/cm^2, the acquisition ranges of sensor 1 are 9.9 and 7.7 km for sea surfaces with wind speeds 0 and 10 m/s, respectively. At these ranges, the circular-polarization signal-to-clutter (S/C) ratios, E/E_W, are 76 and 330, respectively. Therefore, the circular-component clutter background (E_W) attributable to roughness of sea surface is negligibly small. The relation E_V/E_{VW} versus E_V for the sensor at position 2 is shown in Figure 11. The circular sea background E_W is large. Taking $E/E_W = 10$ as the range criterion, the acquisition ranges are 13.9 and 11.5 km for sea surface with wind speeds 0 and 10 m/s, respectively. At these ranges the circular-polarization target irradiances E are 2700 and 1445 fW/cm^2, respectively. The results are listed in Table 1. The circular-component target signature (E) is very strong. These results show that MWIR circular-polarization sensor is feasible for the sea-skimming missile detection in the solar corridor, either for (1) shipboard or (2) interceptor/helicopter-board sensor application. The range of ship defense interest is 7 to 14 km.

Table 1. Acquisition Ranges for the Two Sensors at Positions 1 and 2.

Parameter	Position	Wind Speed (m/s)	
		0	10
Acq. Range (km)	1	9.9	7.7
	2	13.9	11.5
E (fW/cm^2)	1	10	10
at Acq. Range	2	2700	1445
E/E_W	1	76	330
at Acq. Range	2	10	10

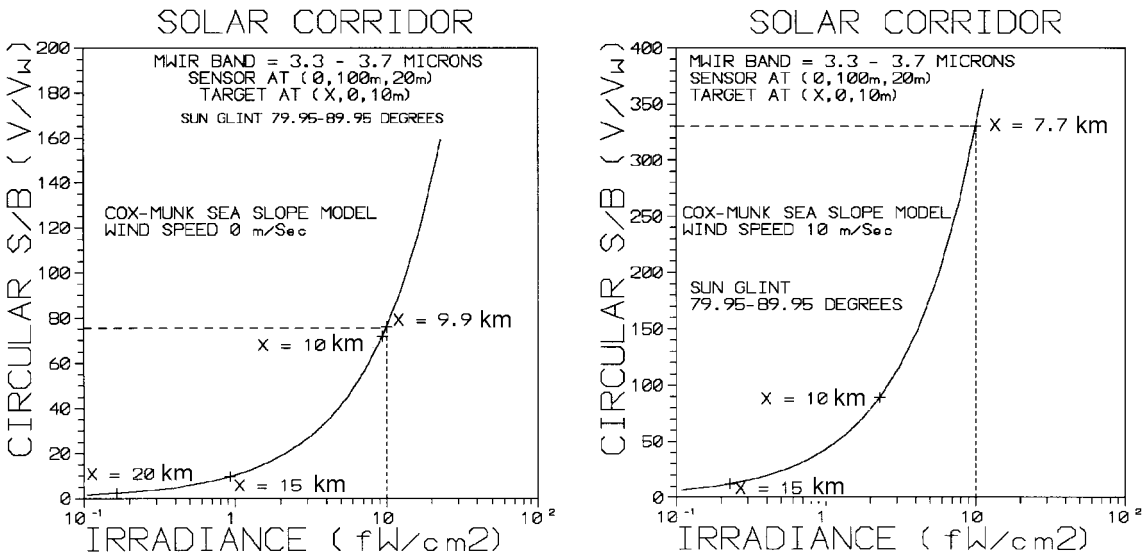

(a) Wind speed 0 m/s. (b) Wind speed 10 m/s.

Figure 10. The E_V/E_{VW} Versus E_V Relation for the Sensor at Position 1. The horizontal ranges X are marked.

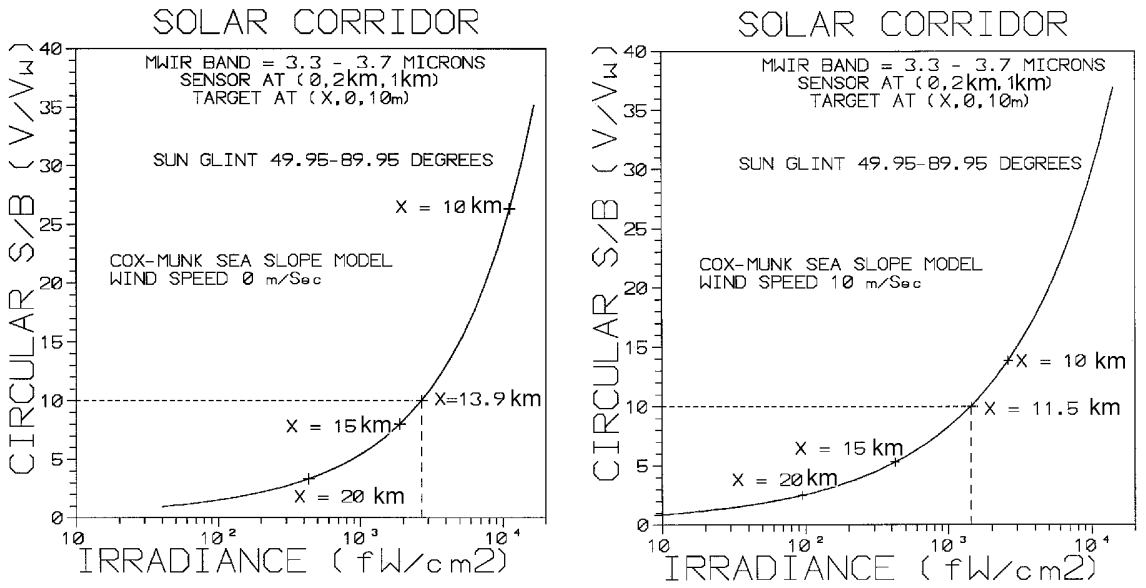

(a) Wind speed 0 m/s. (b) Wind speed 10 m/s.

Figure 11. The E_V/E_{VW} Versus E_V Relation for the Sensor at Position 2. The horizontal ranges X are marked.

III. REALISTIC MODEL OF SHIPBOARD SENSOR PERFORMANCE RESULTS FOR SKIMMING MISSILE DETECTION IN SOLAR CORRIDOR

As shown in Figure 12, instead of a cylinder, we consider a missile model, which includes three parts: (1) 10-m-long, 1-m-diameter cylinder, (2) 0.5-m-long conic head, and (3) 2-m-long, 1-m-diameter plume cylinder. We made the following assumptions:

1. The missile has a surface temperature 320 K for a typical Mach number 0.9 of cruise missile and a painted surface with optical constants 1.5 + i 0.15.
2. The plume cylinder has a temperature 600 K and emissivity 1 (blackbody approximation).
3. The sea water surface has a temperature 283 K and optical constants 1.401 + i0.0094 (at wavelength 3.5 μm)[12].
4. Cox-Munk model sea-surface slope distribution[15] of wind speed 10 m/s, which is also shown in Figure 12.
5. The sensor characteristics: waveband 3.3- to 3.7-μm, instantaneous field of view (IFOV) = 0.5 mR and noise equivalent irradiance/minimum detection irradiance (NEI/MDI) = 0.1/0.6 W/cm^2.
6. The sea-level air temperature is 283 K.

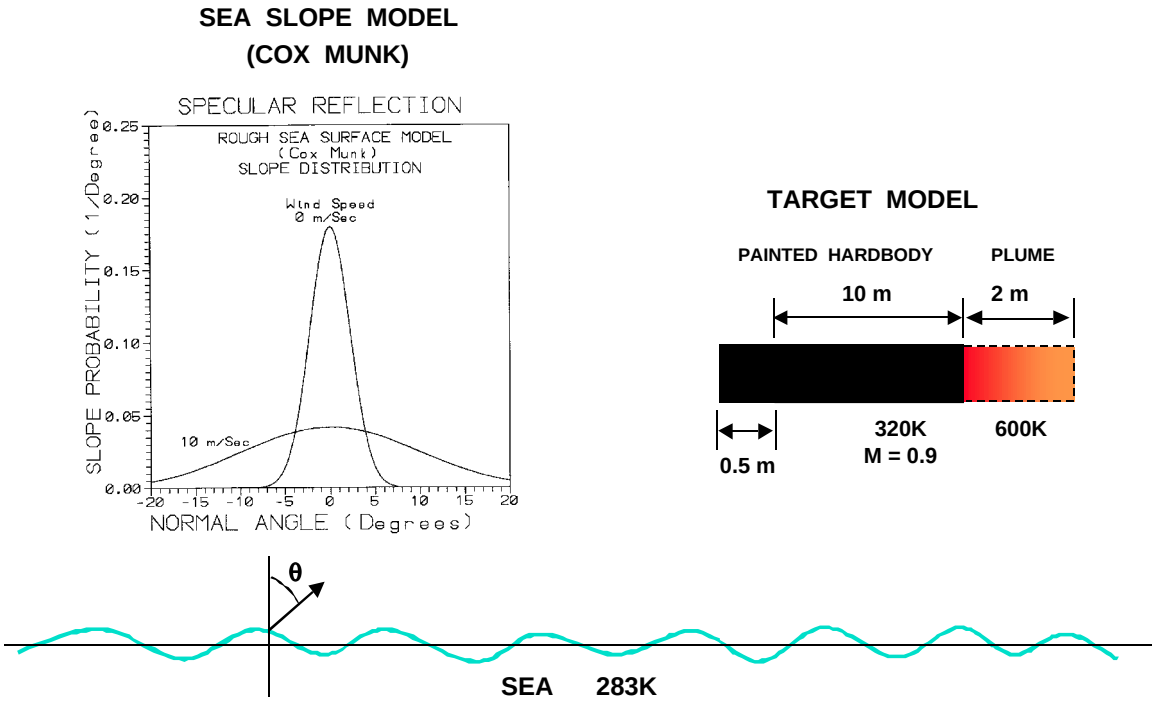

Figure 12. Target and Rough Sea Surface Models.

As shown in Figure 13, we consider the following radiation sources and the (I, V) signals from target and sea background toward the shipboard sensor.

1. Solar glint from the sea will generate I_1 and V_1 signals toward the sensor in the solar corridor.
2. Daylight glint from the sea: I_2 and V_2.
3. Rough-sea emission: I_3 and V_3.
4. Thermal emissions from target and sea surface toward the sensor: I_4.
5. Target reflected air and daylight radiation: I_5.
6. Plume radiation from target: I_6.

For horizontal range 5 to 30 km, the target I-irradiances (1 through 6) and V-irradiances (1 through 3) at the sensor are shown in Figure 14. The rough-sea-background I-irradiances (1 through 4) and V- irradiances (1 through 3) are shown in Figure 15. The sensor MDI [0.6 pW/cm^2] is marked. It shows that the solar glint I-signal of sea background (Figure 15) is much greater than that of target (Figure 14) and also MDI. However, The V-irradiance of the target (Figure 14) is greater than MDI for range less than 15 km. The V-irradiance of the sea-background (Figure 15) is much weaker than MDI/NEI. Therefore, these results provide the physical foundation of detecting a skimming missile in solar corridor.

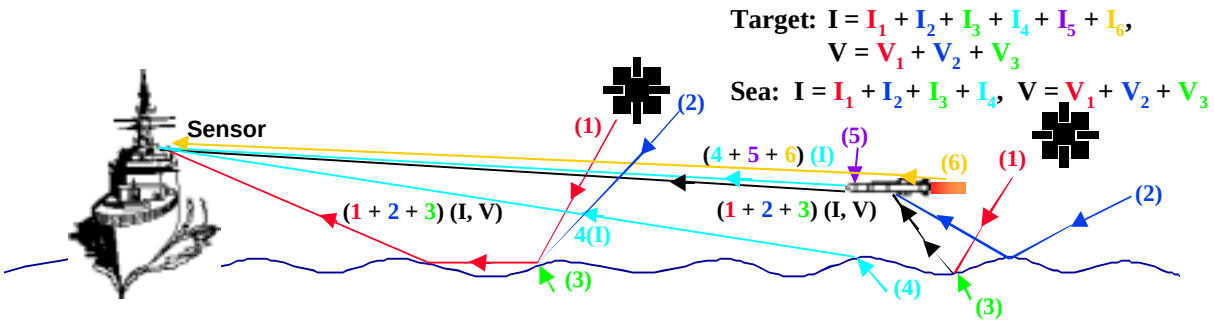

Figure 13. Radiation Sources of Target and Sea Background Signals Toward the Ship-Board Sensor.

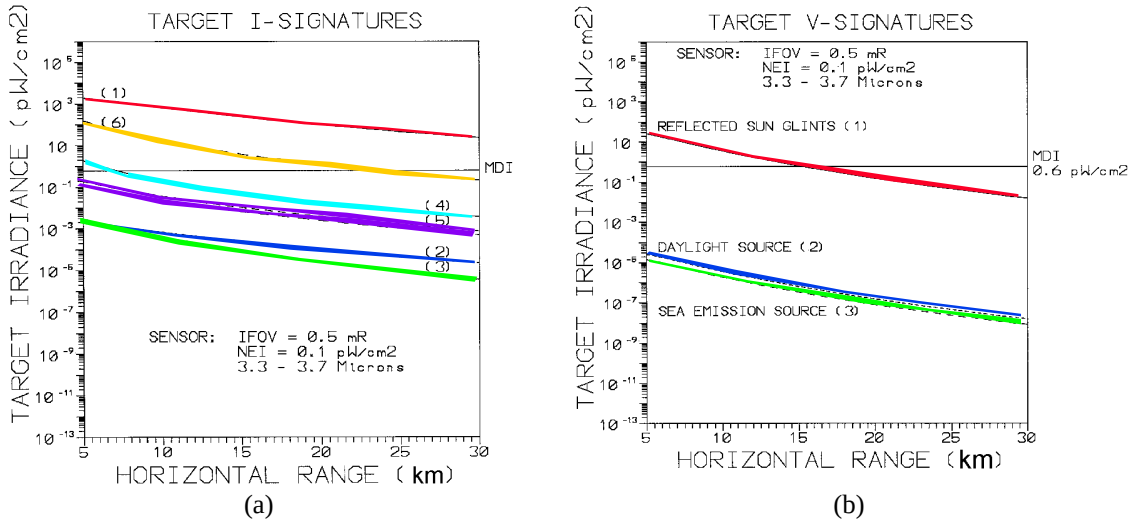

Figure 14. Contributions of Target I- and V- Irradiances Toward the Shipboard Sensor for a Horizontal Range 5 - 30 km.

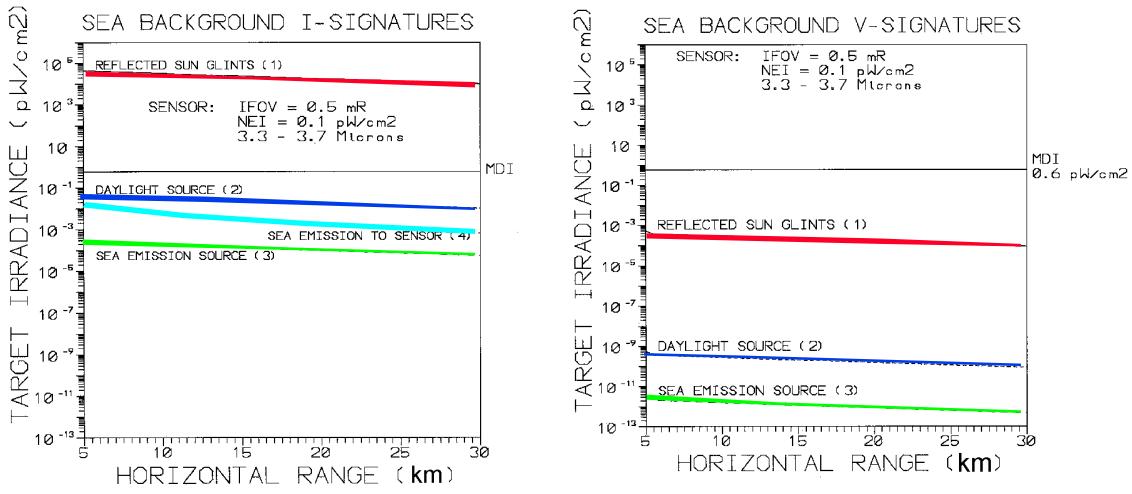

Figure 15. Contributions of Rough-Sea Background I- and V- Irradiances Toward the Shipboard Sensor for a Horizontal Range 5 - 30 km.

The total I and circular V signals detected by the sensor are

<u>In solar corridor</u>			
Target	$I = I_1 + I_2 + I_3 + I_4 + I_5 + I_6$	$V = V_1 + V_2 + V_3$	(5a)
Sea background	$I = I_1 + I_2 + I_3 + I_4$	$V = V_1 + V_2 + V_3$	(5b)
<u>Outside solar corridor</u>			
Target	$I = I_2 + I_3 + I_4 + I_5 + I_6$	$V = V_2 + V_3$	(6a)
Sea background	$I = I_2 + I_3 + I_4$	$V = V_2 + V_3$	(6b)
<u>Night</u>			
Target	$I = I_3 + I_4 + I_5 + I_6$	$V = V_3$	(7a)
Sea background	$I = I_3 + I_4$	$V = V_3$	(7b)

For a horizontal range between 5 and 30 km, the total target I-irradiances and V-irradiances at the sensor are shown in Figure 16. Results shown are (1) in solar corridor (solid curves), (2) outside solar corridor (short broken curves) and (3) night (long broken curves). I is larger than the V. The total rough-sea-background I-irradiances and V-irradiances at the sensor are also shown in Figure 16. A S/C plot is shown in Figure 17. Sensor MDI 0.6 pW/cm^2 and the S/C = 1 and 6 lines are marked.

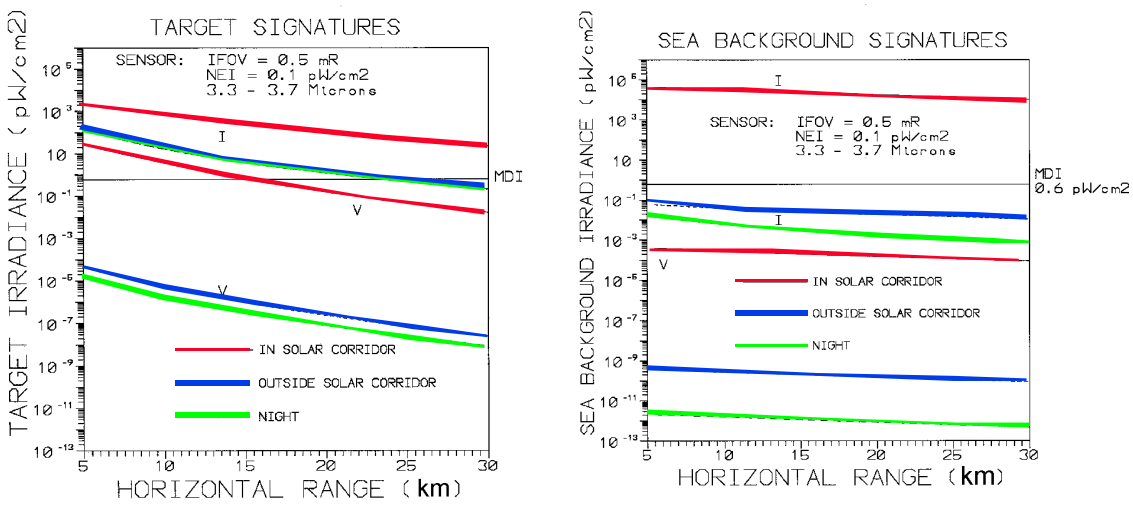

Figure 16. Target and Sea Background I- and V- Irradiances Toward the Ship-Board Sensor for Horizontal Range 5 - 30 km and Three Cases: (1) in Solar Corridor (red), (2) Outside Solar Corridor (blue), and (3) at Night (green).

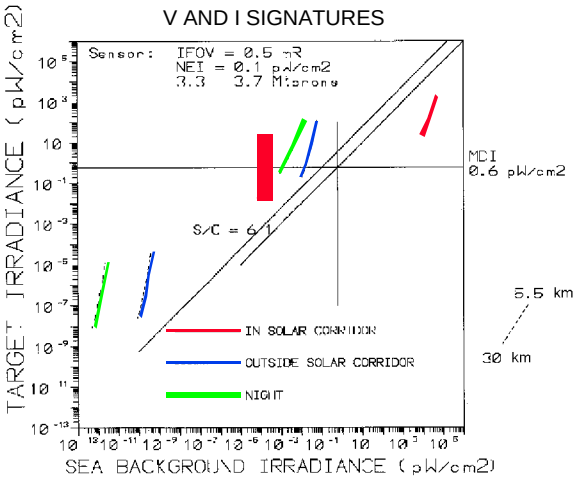

Figure 17. Signal-to-Clutter Plot of the Target and Sea Background I- and V- Irradiances Toward the Shipboard Sensor for Horizontal Range 5.5 - 30 km and Three Cases: (1) in Solar Corridor (red), (2) Outside Solar Corridor (blue), and (3) at Night (green). The lines of MDI = 0.6 pW/cm^2 are marked.

Figures 16 and 17 show the following results:

1. In solar corridor, the I-irradiance of sea background is much greater than that of the target. The V-irradiances of the target are greater than MDI (0.6 pW/cm^2) for a range less than 15 km. The V-irradiances of sea background are much smaller than MDI and cannot be detected. Therefore, it is feasible to use the circular-polarization V-sensor to detect a sea-skimming missile in the solar corridor.

2. Outside the solar corridor or at night, the V-irradiances of the target are much smaller than MDI. The total I-sensor is feasible for detection.

IV. DISCUSSION AND CONCLUSION

We have calculated the polarization signatures of a model sea-skimming target with painted surface. The circular polarization reflection-reflection signatures for the cylinder above the water plane with both flat and rough (Cox-Munk model[15]) sea surface are studied quantitatively. The result shows the feasibility of detecting sea-skimmer targets above the sea surface. In the solar corridor, the sun glints reflected from the water surface and then reflected from a target surface would have significant circular polarization. This reflection is stronger than the reflection background from rough sea surface (Figures 14 and 15). Therefore, a circular-polarization sensor would be feasible as an adjunct sensor for sea-skimming missile detection in the solar corridor when the current intensity-only sensor has difficulty.

The target/background V-irradiance vs. horizontal range (Figure 16) and S/C for V (Figure 17) provides us the curves to determine the sensor sensitivity (MDI/NEI) value needed for the acquisition range requirement. For example, the V-acquisition range would increase from 15 to 20 km, if the sensor MDI decreases from 0.6 to 0.1 pW/cm^2. An acquisition range of 10 km would be acceptable. Therefore, our model sensor with a 3.3- to 3.7-μm waveband, MDI/NEI = 0.6/0.1 pW/cm^2 and IFOV = 0.5 mR has acceptable sensor parameters for detecting sea-skimming missile in the solar corridor.

As shown in Figures 13, 14, and 15, in the solar corridor, the terms attributable to solar glint from the sea—I_1 and V_1—are the dominate signals toward the sensor. These signals are plotted in Figure 18. The curves for smaller IFOV (= 0.2 mR) are also shown. Clutter background is reduced for better sensor resolution IFOV. For a shipboard sensor, a smaller IFOV (0.2 mR) sensor and better sensitivity (MDI < 10 fW/cm^2) represent feasible technology. Therefore, a circular-polarization sensor is feasible for detecting a skimming missile in the solar corridor.

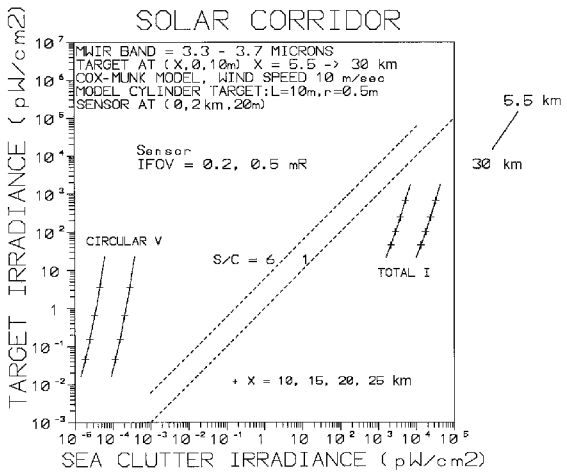

Figure 18. S/C Plot of the Solar Glint Contributed Target and Sea-Background I- and V- Irradiances Toward the Shipboard Sensor for Horizontal Range of 5.5 - 30 km in Solar Corridor and Sensor IFOV = 0.2 and 0.5 mR.

We use the 3.3- to 3.5-μm band wavelength for the V-sensor for two reasons:

1. The circular V-signal is weak. We use the strong solar radiation source to get a target V-irradiance larger than the sensor MDI.
2. Narrow band is usually chosen for the achromatic waveplate of the V-sensor. Therefore, band selection is a key consideration of circular polarization sensor design for the specific mission application.

For night application, the thermal radiation emitted from the sea surface and then reflected from the target would also produce the circular polarization signature for discrimination and tracking. The long-wave infrared (LWIR) would be preferred because of the low water temperature of the sea.

The conclusions are

1. Theory and algebra of circular-polarization signatures of the target have been developed.
2. The circular component of solar glint background reflected from a rough sea surface is negligibly small.
3. Our model V-sensor with 3.3- to 3.7-μm waveband, MDI/NEI = 0.6/0.1 pW/cm^2 and IFOV = 0.5 mR has acceptable parameters for detecting sea-skimming missiles in the solar corridor.
4. Our model I-sensor with the same parameters is feasible for detecting sea-skimming missiles outside the solar corridor or at night.
5. A full-polarization (I, Q, U, V) sensor with these parameters would be feasible for detecting sea-skimming missiles in and out of the solar corridor and at night.
6. The infrared circular-/full-polarization sensor technology is worth development.

ACKNOWLEDGMENT

This research was supported partly by (1) ONR-NAWCWD in-house Laboratory Independent Research Program, (2) NAVSEA TBMD Program, (3) NAWCWD China Lake Discretionary Funds, and (4) ONR ASWT Program.